

Supplementary Material

“Influence of Grain Size on Mechanical Properties of a Refractory High Entropy Alloy under Uniaxial Tension”, Deluigi *et al.*, Crystals (2023)

The Supplementary Material (SM) contains Figures S1 to S8 and a brief explanation of those figures.

Machine learning for identification of grains

Identification of grains and GBs was carried out using Random Forests (RF). By using OVITO and common neighbor analysis (CNA), GB atoms were manually selected using a slice of the sample at 0.24 strain, as shown by the red atoms in Fig.S1. CNA identifies both twins and GBs as *other* atom type, so selection must be performed carefully. A total of 437,411 atoms were involved in this analysis. Grain atoms and GB atoms were used for classification in RF. The following quantities were employed as features: potential energy, coordination number from the radial distribution function, atomic volume from Voronoi analysis, per-atom entropy from pair entropy fingerprint [Piaggi2017], centrosymmetry parameter for bcc and fcc structures [Kelchner1998], and the q_2 , q_4 , q_6 , q_8 Steinhardt order parameters [Steinhardt1983]. All these quantities were calculated before slicing the sample, and they were standardized to diminish the effect of outliers. 80% and 20% of grain and GB atoms (together) were used as training and testing sets, with 500 trees as estimators.

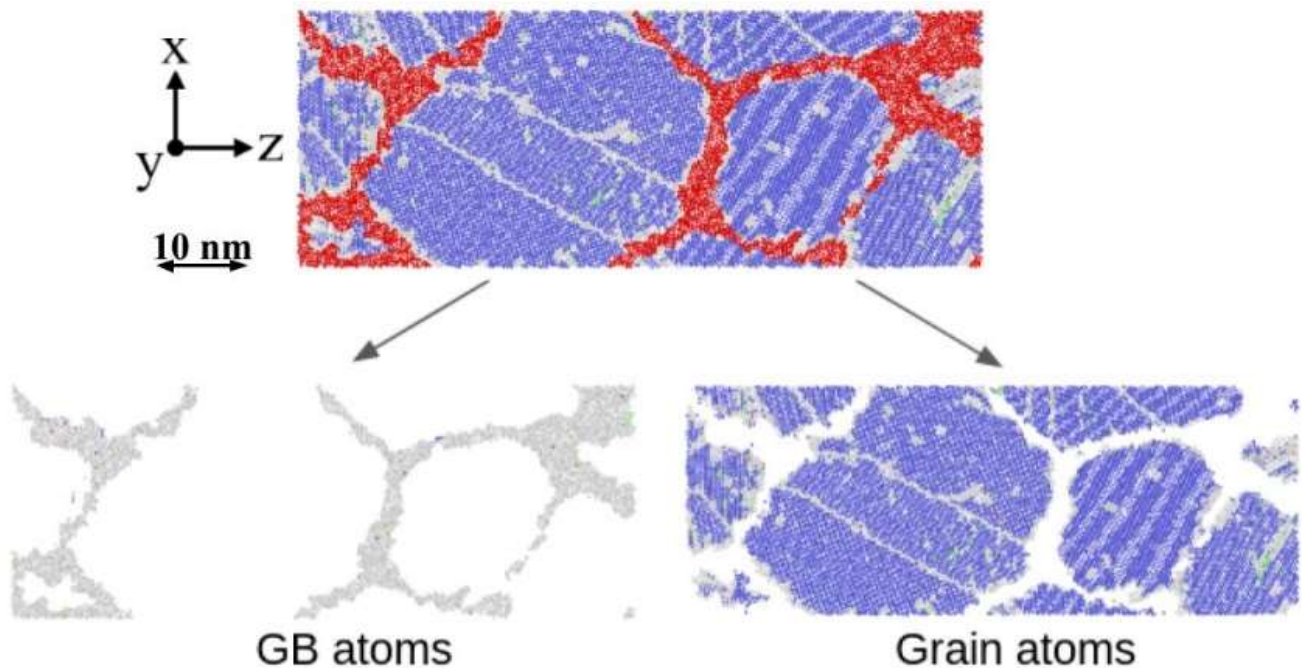


Figure S1. Manual selection of GB atoms and grain atoms at 0.24 strain for the 17 nm sample.

Additional structural and plasticity analysis

Fig. S2 shows radial distribution functions for nc samples at different strains. Fig. S3 shows "Other" atoms versus strain for two different grain sizes. Fig. S4 shows dislocation lines. Figs. S5 and S6 display PTM, shear strain and misorientation for 8 nm and 17 nm samples, with 3D views, complementary to the 2D views in the main text. Fig. S7 focus on the misorientation for the single crystal, at 0.4 strain. Finally, Fig. S8 shows twin volume fraction (TVF), but normalized to the amount of bcc atoms at each strain for each sample.

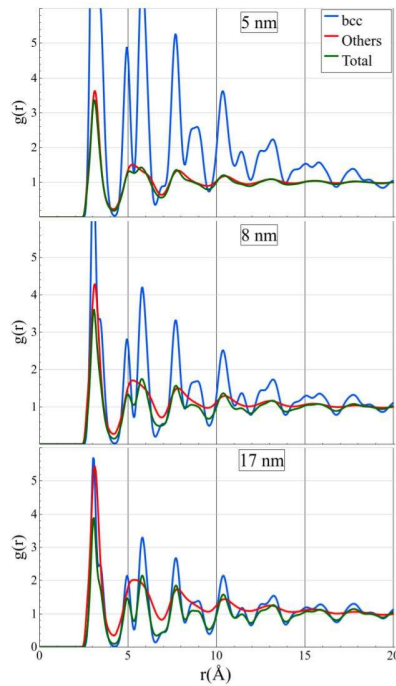


Figure S2. Radial distribution for several grain sizes at 0.4 strain. Each panel includes lines for all atoms ("total"), only bcc atoms, and only atoms type "Other" according to PTM. Since each curve was calculated for a different number of atoms, $g(r)$ was normalized such that its average between $r=18$ and $r=20$ was unity. This causes the bcc peaks to be higher for the small grain samples, where the bcc content is low. As the grain size decreases, $g(r)$ for the entire sample resembles more closely the one for atoms type "Other", evidencing a large fraction of the amorphous GB phase.

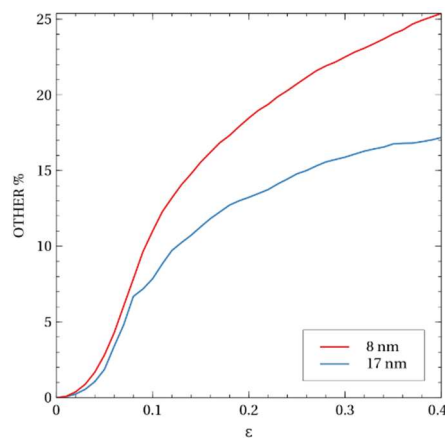


Figure S3. Grain analysis using the Polyhedral Template Matching selection procedure versus strain. The additional fraction of "other"-type atoms in the simulation, taking strain zero as the starting point for structures with 8 and 17 nm grain diameters.

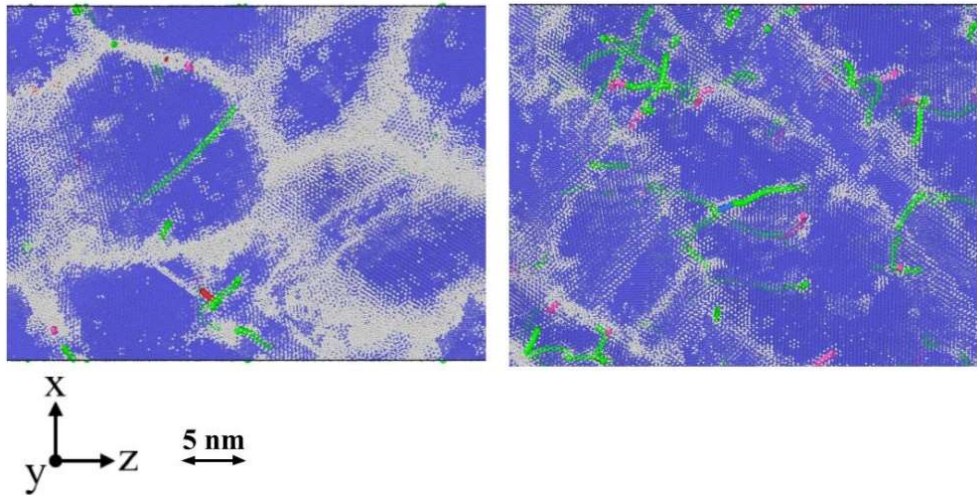


Figure S4. Snapshots at a strain of 0.4, showing dislocations within a 4nm- thick slice of a section of the sample, for the 17 nm nc (left panel) and the single crystal (right panel). Atom coloring by PTM with RMSD=0.1: bcc (blue), "other" (white). Dislocation line coloring: $(1/2)\langle 111 \rangle$ (green), unidentified (red).

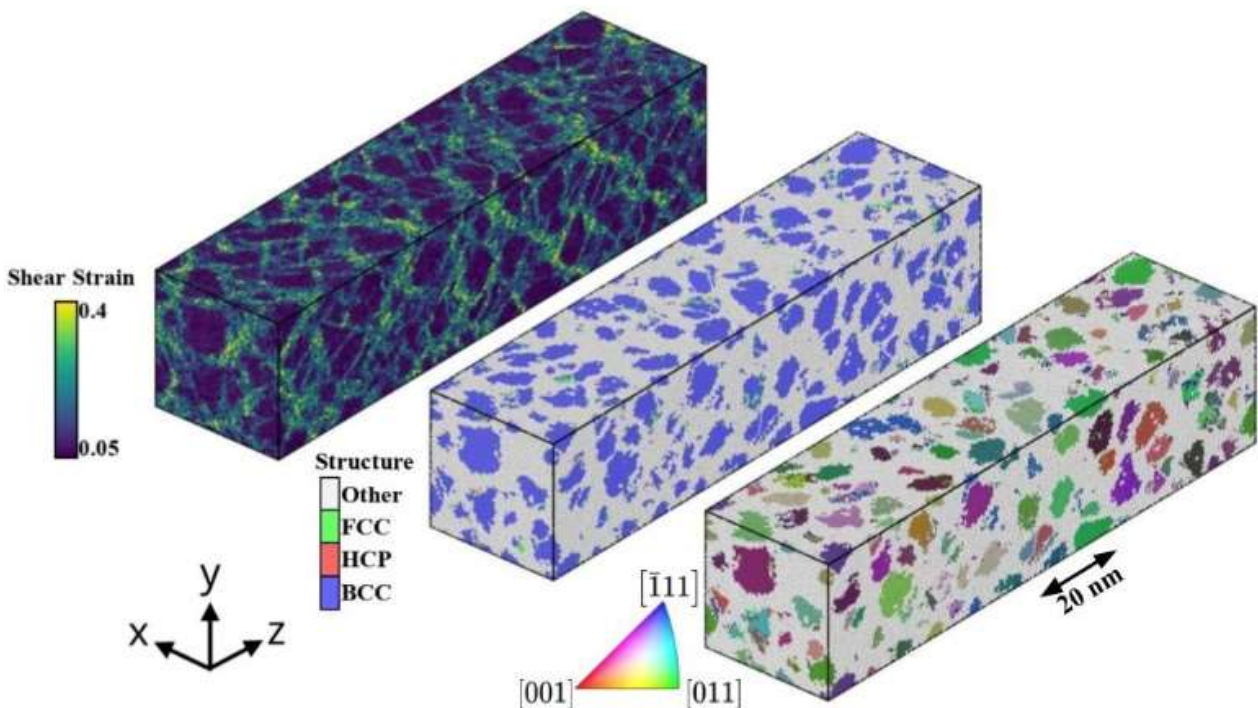


Figure S5. Nanocrystal with $d=8$ nm at 0.4 strain. Left: atomic shear strain, revealing grain boundary plasticity and dislocation glide. Center: Coloring by Polyhedral Template Matching with RMSD=0.1. Right: Grain orientation, relative to the principal low-index axes, as in standard Inverse Polar Figures (IPF). Significant grain rotation and twinning is observed.

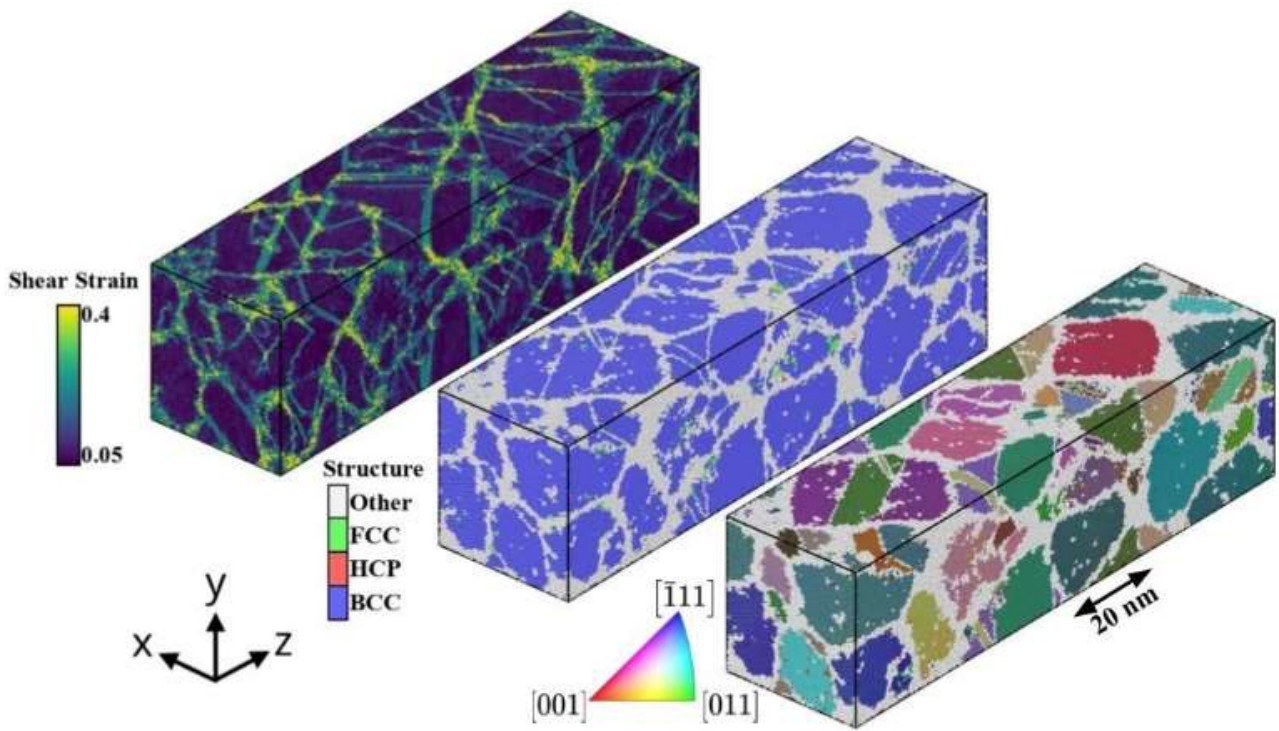


Figure S6. Nanocrystal with $d=17$ nm at 0.4 strain. Left: atomic shear strain, revealing grain boundary plasticity and dislocation glide. Center: Coloring by Polyhedral Template Matching with $\text{RMSD}=0.1$. Right: Grain orientation, relative to the principal low-index axes, as in standard Inverse Polar Figures (IPF). Significant grain rotation and twinning is observed.

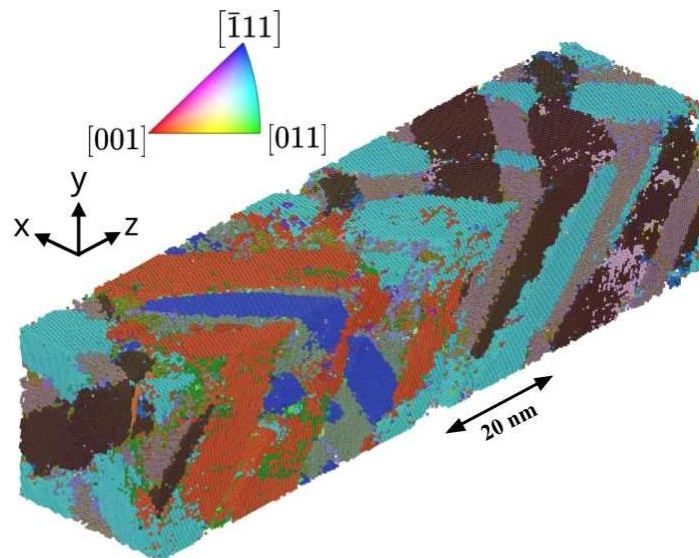


Figure S7. Inverse Polar Figures (IPF) for the single crystal sample deformed along $[001]$, at 0.4 strain. Different colors indicate different crystal orientations due to several twin variants. The original $[001]$ orientation is almost absent.

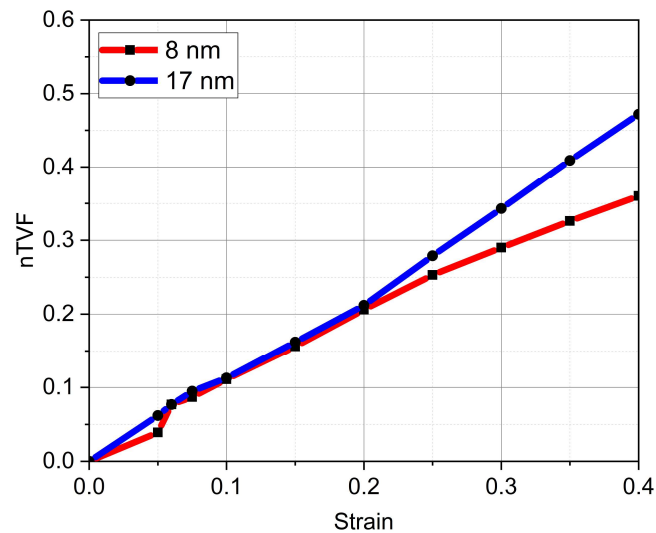


Figure S8. "Normalized" twin volume fraction evolution with strain. Instead of using the total sample volume, as in Fig. 11, the volume of bcc atoms at each strain is considered for the normalization, bringing closer the 8 nm and 17 nm results.

References

- [Piaggi2017] Piaggi, P.M.; Parrinello, M. Entropy based fingerprint for local crystalline order. *The Journal of Chemical Physics* 2017, 147, 114112. <https://doi.org/10.1063/1.4998408>.
- [Steinhardt1983] Steinhardt, P.J.; Nelson, D.R.; Ronchetti, M. Bond-orientational order in liquids and glasses. *Physical Review B* 1983, 28, 784. <https://doi.org/10.1103/PhysRevB.28.784>.
- [Kelchner1998] Kelchner, C.L.; Plimpton, S.J.; Hamilton, J.C. Dislocation nucleation and defect structure during surface indentation. *Phys. Rev. B* 1998, 58, 11085–11088. <https://doi.org/10.1103/PhysRevB.58.11085>.